Cell Stem Cell. Author manuscript; available in PMC 2013 December 09.

Published in final edited form as:
Cell Stem Cell. 2010 June 4; 6(6): . doi:10.1016/j.stem.2010.04.002.

CNS-Resident Glial Progenitor/Stem Cells Produce Schwann Cells as well as Oligodendrocytes during Repair of CNS Demyelination

Malgorzata Zawadzka[1,2], **Leanne E. Rivers**[3,4], **Stephen P.J. Fancy**[1,6], **Chao Zhao**[1], **Richa Tripathi**[3,4], **Françoise Jamen**[3,8], **Kaylene Young**[3,4], **Alexander Goncharevich**[1], **Hartmut Pohl**[7], **Matteo Rizzi**[3,5], **David H. Rowitch**[6], **Nicoletta Kessaris**[3,4], **Ueli Suter**[7], **William D. Richardson**[3,4,*], and **Robin J.M. Franklin**[1,*]

[1]MRC Cambridge Centre for Stem Cell Biology and Regenerative Medicine and Department of Veterinary Medicine, University of Cambridge, Madingley Road, Cambridge CB3 0ES, UK [2]Laboratory of Transcription Regulation, Department of Cell Biology, Nencki Institute of Experimental Biology, 3 Pasteur Str., 02-093 Warsaw, Poland [3]Wolfson Institute for Biomedical Research University College London, Gower Street, London WC1E 6BT, UK [4]Research Department of Cell and Developmental Biology University College London, Gower Street, London WC1E 6BT, UK [5]Research Department of Neuroscience, Physiology and Pharmacology University College London, Gower Street, London WC1E 6BT, UK [6]Howard Hughes Medical Institute and Institute for Regeneration Medicine, Department of Pediatrics, University of California San Francisco, 513 Parnassus Avenue, San Francisco, CA 94143, USA [7]Institute of Cell Biology, Department of Biology, ETH Zurich, CH-8093 Zurich, Switzerland

SUMMARY

After central nervous system (CNS) demyelination—such as occurs during multiple sclerosis—there is often spontaneous regeneration of myelin sheaths, mainly by oligodendrocytes but also by Schwann cells. The origins of the remyelinating cells have not previously been established. We have used Cre-lox fate mapping in transgenic mice to show that PDGFRA/NG2-expressing glia, a distributed population of stem/progenitor cells in the adult CNS, produce the remyelinating oligodendrocytes and almost all of the Schwann cells in chemically induced demyelinated lesions. In contrast, the great majority of reactive astrocytes in the vicinity of the lesions are derived from preexisting FGFR3-expressing cells, likely to be astrocytes. These data resolve a long-running debate about the origins of the main players in CNS remyelination and reveal a surprising capacity of CNS precursors to generate Schwann cells, which normally develop from the embryonic neural crest and are restricted to the peripheral nervous system.

INTRODUCTION

The adult CNS does not usually regenerate efficiently after mechanical injury or degenerative disease. However, the remyelination that follows destruction of central myelin is an exception to this rule and provides a striking example of stem/precursor cell-mediated

*Correspondence: w.richardson@ucl.ac.uk (W.D.R.), rjf1000@cam.ac.uk (R.J.M.F.).
[8]Present address: CNRS Institut de Neurobiologie Alfred Fessard, 91198 Gif-sur-Yvette, France

SUPPLEMENTAL INFORMATION Supplemental Information includes four figures and one movie and can be found with this article online at doi:10.1016/j.stem.2010.04.002.

Europe PMC Funders Author Manuscripts

regeneration. Remyelination involves the generation of new myelin-forming glia that elaborate multilamellar myelin sheaths around denuded axons, restoring saltatory conduction and conferring axonal protection (Franklin and ffrench-Constant, 2008).

CNS remyelination is usually mediated by oligodendrocytes and can occur efficiently and extensively after experimentally induced demyelination in animal models or during demyelinating diseases such as multiple sclerosis (MS), the most common neurological disease of young adults (Patrikios et al., 2006). CNS remyelination can also be mediated by Schwann cells, the myelin-forming cells of the peripheral nervous system; this occurs in several experimental animal models of demyelination as well as in human demyelinating disease (Dusart et al., 1992; Felts et al., 2005; Itoyama et al., 1983, 1985; Snyder et al., 1975). Schwann cell remyelination occurs preferentially where astrocytes are absent—for example, where they have been killed along with oligodendrocytes by the demyelinating agent (Blakemore, 1975; Itoyama et al., 1985). Failure of remyelination in progressive MS is associated with secondary axonal loss, which leads to the untreatable clinical deterioration that often characterizes late-stage MS (Trapp and Nave, 2008).

The cellular origins of remyelinating oligodendrocytes and Schwann cells in the CNS have not been formally resolved. Mature oligodendrocytes within the spared white matter surrounding demyelinated lesions appear not to contribute to remyelination (Keirstead and Blakemore, 1997). Instead, it is generally believed that most remyelinating oligodendrocytes are derived from adult oligodendrocyte precursors (OLPs, also known as NG2 cells). These cells, typically identified by their expression of the proteoglycan NG2 and the platelet-derived growth factor receptor (alpha subunit, PDGFRA) (Nishiyama et al., 1996; Pringle et al., 1992), are widespread throughout the CNS, comprising ~5% of all cells in the adult rodent CNS (Nishiyama et al., 1996; Pringle et al., 1992). Recently, it has been shown by Cre-lox fate mapping that OLPs continue to generate new myelinating oligodendrocytes in the healthy adult mouse brain for at least 8 months after birth (Dimou et al., 2008; Rivers et al., 2008). The evidence that OLPs are the major source of remyelinating oligodendrocytes after demyelination is indirect but compelling: (1) retroviral or BrdU/autoradiographic tracing indicates that dividing cells in adult white matter (likely but not proven to be adult OLPs) give rise to remyelinating oligodendrocytes (Gensert and Goldman, 1997; Watanabe et al., 2002), (2) remyelination can be achieved by transplanted OLPs (Zhang et al., 1999), (3) demyelinating lesions are repopulated by OLPs prior to the appearance of remyelinating oligodendrocytes (Sim et al., 2002b), and (4) cells expressing molecular markers of both OLPs and oligodendrocytes can be identified at the onset of remyelination (Fancy et al., 2004).

In contrast, remyelinating Schwann cells within the CNS are generally thought to migrate into the CNS from PNS sources such as spinal and cranial roots, meningeal fibers, or autonomic nerves after a breach in the glia limitans (Franklin and Blakemore, 1993). In support of this idea, CNS Schwann cell remyelination typically occurs in proximity to spinal/cranial nerves or around blood vessels (Duncan and Hoffman, 1997; Sim et al., 2002a; Snyder et al., 1975). However, the ability of CNS precursors to generate Schwann cells in vitro and after transplantation into the demyelinated CNS raises the possibility that some CNS Schwann cell remyelination might result from unusual differentiation of endogenous CNS precursors (Keirstead et al., 1999; Mujtaba et al., 1998).

In this study, we used genetic fate mapping with a battery of Cre transgenic mice to investigate the cellular origins of the new oligodendrocytes, Schwann cells, and astrocytes that develop in and around toxin-induced demyelinated lesions. We show (1) that PDGFRA- and OLIG2-expressing precursors (OLPs) give rise to all remyelinating oligodendrocytes, (2) that the majority of remyelinating Schwann cells within the CNS are also derived from

OLPs, not P_0-expressing Schwann cells in the PNS, and (3) that the great majority of newly generated reactive astrocytes (but not oligodendrocytes or Schwann cells) are derived from FGFR3-expressing cells, most likely preexisting astrocytes. Collectively, these data provide a detailed account of the cellular origins of the macroglial cells that reconstruct areas of CNS white matter demyelination.

RESULTS

Efficient Labeling of PDGFRA-Expressing Cells after Lysolecithin-Induced Demyelination

By using *Pdgfra-creER^{T2}:Rosa26-YFP* mice, which allow tamoxifen-inducible expression of yellow fluorescent protein (YFP) in PDGFRA$^+$ precursor cells and all of their progeny (Rivers et al., 2008), we asked whether the YFP reporter was expressed in OLPs that repopulate areas of lysolecithin-induced demyelination in spinal cord white matter. Tamoxifen was administered to *Pdgfra-creER^{T2}:Rosa26-YFP* mice starting on postnatal day 75 (P75), lysolecithin lesions were induced on ~P85, and YFP immunohistochemistry (IHC) was performed on tissue sections 6 days postlesion induction (dpl), when there are many OLPs within the lesion but not yet any differentiated oligodendrocytes (Figure S1A available online; Arnett et al., 2004). The lesioned area contained abundant YFP$^+$ cells, which were confirmed to be OLPs by colabeling for OLIG2, PDGFRA, and NG2 (Figure 1). At 4 dpl, all YFP$^+$ cells within the lesion were positive for transcription factor OLIG2 (Figure S1B) and for NG2 (data not shown), consistent with previous reports (Ligon et al., 2006). We estimated the efficiency of YFP labeling (fraction of PDGFRA-positive cells that were also YFP immunopositive) to be 39% ± 7% (data not shown). The fraction of the OLIG2$^+$ population that was also YFP$^+$ in these animals was 32% ± 9% and this did not change significantly at longer survival times (Figure S1C).

Adult OLPs Generate Remyelinating Oligodendrocytes

To establish whether YFP$^+$ OLPs differentiated into remyelinating oligodendrocytes, sections from 21 day lesions, when remyelination is complete, were examined by double IHC with YFP and either CC1 or Transferrin, two markers of differentiated oligodendrocytes. Abundant YFP$^+$/CC1$^+$ and YFP$^+$/Transferrin$^+$ cells were evident within the outer rim of the lesion, where oligodendrocyte-mediated remyelination can be detected by histology (Figure 2; Figure S2). Within the YFP$^+$ population at 14 dpl, 32% ± 7% of cells were CC1$^+$ (at a density of 167 ± 36 cells/mm^2) and 11% ± 2% were Transferrin$^+$, while at 21 dpl 45% ± 6% (346 ± 50 cells/mm^2) were CC1$^+$ and 24% ± 3% were Transferrin$^+$ (Figure 2C). In spinal cord white matter, all Transferrin$^+$ cells were also CC1$^+$ (data not shown). None of the CC1$^+$ or Transferrin$^+$ oligodendrocytes in surrounding intact tissue expressed YFP. However, we did find occasional YFP$^+$ cells of oligodendrocyte morphology expressing CC1 in the normal appearing white matter remote from the lesion and in intact gray matter (data not shown), consistent with our earlier findings (Rivers et al., 2008). To show that YFP$^+$ cells at 21 dpl were associated with myelin sheaths, longitudinal spinal cord sections were cut from previously demyelinated tissue and stained for YFP and the myelin proteolipid protein (PLP). YFP is sterically excluded from compact myelin, but there was a clear association between YFP$^+$ cytoplasmic processes/channels and PLP$^+$ compacted myelin (Figure 2D). Finally, we were able to identify YFP$^+$ cells with distinctive myelinating oligodendrocyte morphology when they were dye-filled by electroporation, thereby providing further direct evidence that *Pdgfra*-expressing precursors give rise to remyelinating oligodendrocytes (Figure 2E; Movie S1). We found little evidence for generation of neurons within repairing white matter lesions, although rare DCX$^+$/YFP$^+$ cell bodies were observed (<0.01% of YFP$^+$ cells). These findings indicate that adult OLPs are able to differentiate into myelin-forming oligodendrocytes after CNS demyelination.

Oligodendrocyte Precursor Cells Differentiate into Remyelinating Schwann Cells

Consistent with previous descriptions of remyelination after toxin-induced demyelination, we observed Schwann cell remyelination in the center of lysolecithin-induced lesions, which were typically devoid of astrocytes, whereas oligodendrocyte remyelination occurred in astrocyte-containing regions around the lesion edge (Blakemore, 1975; Talbott et al., 2005; Woodruff and Franklin, 1999). We asked whether OLPs can contribute to this Schwann cell remyelination in *Pdgfra-creER^{T2}*: *Rosa26-YFP* mice. At 14–21 dpl, when oligodendrocyte and Schwann cell myelin sheaths are present, we found clusters of YFP$^+$ cells that did not express OLIG2 (Figure 3A; Figure S2B). Many of these YFP$^+$ cells had nuclear expression of the Schwann cell-associated transcription factor SCIP/OCT6. SCIP is expressed by premyelinating Schwann cells and its expression is downregulated at the onset of myelination (Sim et al., 2002a). The fraction of SCIP$^+$ cells that was YFP$^+$ in ventral funiculus lesions ranged from 40% ± 10% at 14 dpl to 24% ± 11% at 21 dpl. Within the same areas of the lesion, many of the YFP$^+$ cells associated with myelin sheaths were positive for Periaxin, a myelin protein expressed in PNS-myelin but not CNS-myelin (Figure 3B; Gillespie et al., 1994). We found that 20% ± 2% of YFP$^+$ cells were Periaxin$^+$ at 14 dpl (which accounts for 35% ± 9% of total number 300 ± 83 Periaxin-positive cells per mm^2) and 29% ± 13% at 21 dpl (31% ± 14% of total 650 ± 250 Periaxin-positive cells per mm^2). These cells had the distinctive morphology of myelinating Schwann cells and were closely associated with axons, identified in longitudinal sections by the anti-neurofilament antibody SMI31 (Figure 3C).

Previous studies have shown that ethidium bromide (EB)-induced demyelinating lesions in the spinal cord differ from lysolecithin-induced lesions by having a greater depletion of astrocytes, associated with a higher proportion of Schwann cell-mediated remyelination (Blakemore and Franklin, 2008). We explored the origin of these remyelinating Schwann cells, by injecting EB solution into the spinal cord white matter of *Pdgfra-creER^{T2}: Rosa26-YFP* mice. At 21 dpl, we found that a significantly higher proportion of YFP$^+$ cells coexpressed Periaxin in EB lesions than in lysolecithin-induced lesions (56% ± 8% which accounts for 36% ± 12% of total 811 ± 250 Periaxin-positive cells per mm^2), whereas the proportion of YFP$^+$ cells that were Transferrin$^+$ oligodendrocytes was similar in both types of lesion (39% ± 4% versus 45% ± 6%, respectively) (Figure 3D). These observations suggested that at least some of the remyelinating Schwann cells in both types of lesion were derived from PDGFRA$^+$ OLPs.

An alternative explanation for the findings described above is that Schwann cells in the PNS upregulate *Pdgfra* (and hence CreER^{T2}) in response to nearby injury in the CNS and that these cells then migrate into the demyelinated CNS. To test this possibility, we induced activation of the PNS by performing a sciatic nerve crush injury in *Pdgfra-creER^{T2}*: *Rosa26-YFP* mice. At 6 days after injury, we were able to detect *Pdgfra* transcripts by RT-PCR of mRNA isolated from injured nerve and also found many YFP$^+$ cells at the injury site. However, none of these cells colabeled with the Schwann cell lineage markers, SCIP/OCT6, S100, p75, or Periaxin. The same was also true at 21 dpl, when axon regeneration was advanced. Instead, the YFP$^+$ cells colabeled with fibronectin and were therefore likely to be cells of the connective tissue elements of the peripheral nerve (Figure 4; Raivich and Kreutzberg, 1987).

As a further test of the idea that remyelinating Schwann cells in the CNS are centrally derived, we used an *Olig2-cre* transgenic line (Kessaris et al., 2006) (see Experimental Procedures). Note that this line expresses a constitutively active version of Cre, so that all the descendants of *Olig2*-positive precursors in the embryo and adult are labeled, including motor neurons, mature oligodendrocytes, and adult OLPs, as well as a subset of fibrous and protoplasmic astrocytes (H.-H. Tsai and D.H.R., unpublished observations) (Masahira et al.,

2006). We first demonstrated that, in contrast to *Pdgfra*, there was no expression of *Olig2* mRNA in normal or crushed peripheral nerve, confirming that *Olig2* expression is confined to the CNS (Figure 4). Similarly, we did not observe YFP expression in any cells (apart from some axons) after sciatic nerve crush in *Olig2-cre: Rosa26-YFP* mice, confirming that Olig2 is not expressed within peripheral glia even after injury (Figure 5C). However, we found numerous YFP^+ cell bodies associated with $Periaxin^+$ myelin sheaths within remyelinated spinal cord lesions in *Olig2-cre: Rosa26-YFP* mice at 21 dpl, suggesting that remyelinating Schwann cells in the CNS were derived from CNS precursors (Figures 5A and 5B).

If Schwann cells come from CNS precursors, we predict that it should be possible to identify transitional cells that coexpress markers of both CNS and PNS myelinating lineages. Because many of the antibodies needed to test this prediction were raised in mouse, we instead examined lesions in rat CNS, made either in the caudal cerebellar peduncles by injection of ethidium bromide (Woodruff and Franklin, 1999) or in spinal cord white matter by injection of lysolecithin (Blakemore, 1975). At 7 dpl, shortly before both oligodendrocyte and Schwann cell remyelination commences in these models, approximately half (56% ± 8%) of the $SCIP^+$ cells also expressed Nkx2.2 (normally expressed by oligodendrocytes but not Schwann cells), whereas at 10 dpl, when new myelin sheaths are evident, the proportion had decreased (23% ± 10%) (Figure S3). This supports the conclusion that at least some of the remyelinating Schwann cells are CNS derived.

Few Remyelinating Schwann Cells in the CNS Are Derived from P_0-Expressing Schwann Cells in Peripheral Nerves

Our data provide strong evidence that remyelinating Schwann cells within the CNS can be derived from $PDGFRA^+/OLIG2^+$ CNS precursor cells. However, this does not exclude the possibility that a subset of remyelinating Schwann cells might also be derived from preexisting Schwann cells associated with peripheral nerves of, for example, the spinal roots, meningeal sensory fibers, or autonomic fibers associated with larger blood vessels. To test this, we used a mouse line in which $CreER^{T2}$ is expressed under transcriptional control of the promoter of the peripheral myelin-associated gene P_0, allowing us to prelabel P_0-expressing Schwann cells in *P_0-creER^{T2}: Rosa26-YFP* mice by tamoxifen administration prior to inducing focal demyelination in the dorsal or ventral spinal cord white matter. A high proportion (83% ± 2%) of Periaxin-positive Schwann cells within dorsal and ventral roots were labeled with YFP in these mice (Figure 6A). However, very few Periaxin/YFP double-labeled Schwann cells were found in the spinal cord within ventral white matter lysolecithin lesions (7% ± 2.6% of total $Periaxin^+$ cells); the few $YFP^+/Periaxin^+$ cells identified were at the edges of the lesioned white matter and usually associated with disruption of the meningeal membranes. Within dorsal funiculus lesions, where there was no overt disruption of the integrity of the dorsal aspect of the spinal cord, none of the $Periaxin^+$ cells colabeled with YFP (Figures 6B and 6C). Taken together, our data indicate that although P_0^+ Schwann cells can contribute to Schwann cell-mediated remyelination of the CNS, the great majority of Schwann cell-derived myelin internodes in remyelinated lesions are of CNS origin (Figure 6D).

Most Astrocytes within Remyelinated Lesions Are Derived from FGFR3-Expressing Cells

In addition to remyelinating cells, there is also generation of new astrocytes within areas of lysolecithin-induced demyelination. We asked whether astrocytes within repaired lesions were derived from OLPs, because these cells are known to be able to differentiate into astrocytes in vitro (Raff et al., 1983) and in brain injury (Cassiani-Ingoni et al., 2006). We identified astrocytes by immunolabeling for Aquaporin-4 (AQP4), a transmembrane water channel protein that is expressed in the CNS mainly by astrocytes (Nagelhus et al., 1998).

Glial fibrillary acidic protein (GFAP), a more commonly used marker of fibrous astrocytes, is also expressed by premyelinating Schwann cells in repairing lysolecithin-induced lesions. Examination of lesions induced in *Pdgfra-creER^{T2}: Rosa26-YFP* mice at 21 dpl revealed a small number of YFP$^+$/AQP4$^+$ cells (~3%), usually on the outer rim of the lesion area, indicating that some astrocytes within the lesion were derived from *Pdgfra-creER^{T2}*-expressing precursors (Figure 7A). However, the majority of astrocytes were evidently of a different origin. Given the ability of adult astrocytes to undergo cell division, we hypothesized that newly generated astrocytes might be derived by proliferation of preexisting astrocytes (Buffo et al., 2008; Chen et al., 2008). Adult astrocytes can be identified by the expression of FGFR3 (which is also expressed by cells in the ependymal zone [EZ] associated with the spinal cord central canal), so in order to test this hypothesis, lesions were induced in homozygous *Fgfr3-icreER^{T2}:Rosa26-YFP* mice, in which astrocytes and EZ cells are YFP labeled after tamoxifen administration (Young et al., 2010). Examination of lysolecithin-induced dorsal and ventral lesions at 21 dpl revealed that 96% ± 3% of YFP$^+$ cells expressing AQP4$^+$ (which comprises virtually all AQP4$^+$ cells within the lesion area) and 93% ± 5% of those cells expressing GFAP$^+$ throughout the repaired area, indicating that the majority of astrocytes associated with lesion repair were derived from *Fgfr3*-expressing cells (Figure 7B). However, we did not find any YFP$^+$ cells that also immunolabelled for OLIG2 (Figure S4), CC1, or Periaxin, so it appears that *Fgfr3*$^+$ cells do not generate remyelinating oligodendrocytes or Schwann cells. These data indicate that most reactive astrocytes in demyelinated lesions derive from local astrocytes, not OLPs.

DISCUSSION

White matter injury involving loss of glia with preservation of axons has the capacity to undergo complete cytoarchitectural reconstruction with restoration of the glial compartment. This process can involve the generation of new astrocytes and myelinating cells. Lesions of CNS white matter that involve loss of both astrocytes and oligodendrocytes can be reconstructed so that they resemble peripheral nerve, with the axons remyelinated by Schwann cells in the absence of astrocytes (Blakemore, 1975; Itoyama et al., 1985). Despite the fact that demyelination/remyelination in rodents has been much studied as a model for human disease, the origins of the glial cells that contribute to the process of reconstruction have not been unambiguously defined. In this study we have used genetic lineage tracing strategies to define the origins of oligodendrocytes, astrocytes, and Schwann cells after the induction of focal white matter lesions.

A body of previous work has provided evidence—indirect but persuasive—that remyelinating oligodendrocytes are derived from adult OLPs/NG2 cells (Franklin and ffrench-Constant, 2008). Our present study provides direct and unequivocal confirmation of that conclusion, by genetic fate-mapping in transgenic mice. Although we have demonstrated that *Pdgfra*-expressing OLPs generate many remyelinating oligodendrocytes, we cannot conclude that OLPs are the only source. It remains possible, though less likely than before, that surviving mature oligodendrocytes might synthesize a subset of new myelin internodes. We found no evidence that remyelinating cells are derived from *Fgfr3*-expressing cells—either parenchymal astrocytes or stem/progenitor cells from the EZ around the central canal. We conclude that *Pdgfra*$^+$ precursor cells in the parenchyma are the primary source of remyelinating oligodendrocytes in the mouse spinal cord.

It has been generally assumed that the Schwann cells that myelinate CNS axons are derived from PNS Schwann cells that migrate into the CNS after disruption of the astrocytic glia limitans (Franklin and Blakemore, 1993). This is an attractive hypothesis because Schwann cell remyelination occurs in areas where astrocytes are absent and is more extensive when lesions are located close to a peripheral nerve source (Duncan and Hoffman, 1997; Snyder et

al., 1975). Schwann cell remyelination after EB-induced demyelination in the spinal cord is greater when the lesion is close to spinal roots and meningeal nerves than when it is more remote from the PNS, for example when it is within the cerebellar peduncles (Sim et al., 2002a). Schwann cell remyelination typically occurs around blood vessels, suggesting that the remyelinating Schwann cells might derive from autonomic nerve fibers associated with larger vessels (Sim et al., 2002a) and might use the extracellular matrix-rich environment around vessels as a substrate for migration. It has been reported, for example, that transplanted Schwann cells spread though the CNS along blood vessels (Baron-Van Evercooren et al., 1996). However, apparently pure preparations of CNS stem/precursor cells transplanted into areas of EB-induced demyelination can give rise to remyelinating Schwann cells (Chandran et al., 2004; Keirstead et al., 1999). In this study, we provide evidence that endogenous *Pdgfra*$^+$ and *Olig2*$^+$ cells, very likely representing the same population of CNS stem/precursor cells, efficiently generate remyelinating Schwann cells. Very few, if any, remyelinating Schwann cells in the CNS were derived from cells with a prior history of P_0 expression—implying that myelinating Schwann cells rarely invade the remyelinating spinal cord from the PNS, either directly or after dedifferentiation to P_0-negative Schwann cell precursors. It is thought that many of the remyelinating Schwann cells that are found in regenerating peripheral nerves might be derived from "nonmyelinating Schwann cells" that reside within the nerves; these cells can express low levels of P_0 (Lee et al., 1997) and therefore might also be expected to label in our *P_0-creER^{T2}: Rosa26-YFP* mice. If so, our data suggest that they make only a small contribution to Schwann cell-mediated CNS remyelination. However, because we cannot be sure that nonmyelinating Schwann cells normally express the *P_0-creER^{T2}* transgene at levels high enough to trigger recombination, we cannot exclude the possibility that these cells make a contribution to central remyelination. In a different context, it will be interesting to discover the extent to which either CNS precursors or PNS Schwann cells contribute to the extensive Schwann cell remyelination that follows traumatic injury to the spinal cord.

What could cause CNS-resident precursors to become Schwann cells, which are normally found only in the PNS? One possibility is that a subset of CNS precursors are intrinsically programmed to follow a "neural crest" pathway of development. We are not aware of any data that support this idea other than reports of cells with a Schwann cell-like morphology within the normal CNS (Gudiño-Cabrera and Nieto-Sampedro, 2000). Alternatively, CNS precursors might be exposed to a specific microenvironment within demyelinated lesions that induces ectopic Schwann cell differentiation. Conceivably, this might be triggered by members of the bone morphogenetic protein (BMP) family because pretreating adult OLPs with BMPs in vitro prior to transplantation into demyelinating spinal cord resulted in enhanced Schwann cell remyelination (Crang et al., 2004). Conversely, engineering CNS precursors to overexpress Noggin, an inhibitor of BMP signaling, inhibited Schwann cell differentiation after CNS transplantation (Talbott et al., 2006). Astrocytes have been reported to secrete Noggin (Kondo and Raff, 2004), potentially explaining why the absence of astrocytes in demyelinated lesions might favor Schwann cell differentiation.

The implications of Schwann cell remyelination of CNS axons are unclear. Although both Schwann cell and oligodendrocyte remyelination are associated with a return of saltatory conduction (Smith et al., 1979), their relative abilities to promote axon survival, a major function of myelin (Nave and Trapp, 2008), have yet to be established. Thus, from a clinical perspective, we do not yet know whether OLP differentiation into Schwann cells has a beneficial or deleterious effect compared to oligodendrocyte remyelination.

In the final part of this study, we investigated the origin of newly generated astrocytes that repopulate the periphery of lesions where oligodendrocyte remyelination predominates. OLPs can be induced to generate GFAP$^+$ cells in vitro (Raff et al., 1983) and there is some

evidence that this differentiation pathway is followed during normal development and adulthood (Levison and Goldman, 1993; Zhu et al., 2008). In our study we found that a small proportion of newly generated astrocytes in lesions were derived from *Pdgfra*$^+$-expressing cells. It has been reported that differentiation of OLPs into astrocytes after brain injury is associated with the translocation of OLIG2 from nucleus to cytoplasm (Magnus et al., 2007). However, this observation might simply reflect transient expression of OLIG2 by preexisting astrocytes that are induced to proliferate and/or dedifferentiate in response to injury (Chen et al., 2008). We also cannot exclude the possibility that some proliferating astrocytes might transiently express *Pdgfra*. The overwhelming majority, however, descend from *Fgfr3*$^+$ cells. *Fgfr3* is expressed by two distinct cell populations within the spinal cord—astrocytes and putative stem/progenitor cells around the central canal (Young et al., 2010). However, given that parenchymal astrocytes can divide in response to injury, it seems probable that many of the newly generated astrocytes (identified by expression of AQP4) are derived from local, proliferating astrocytes rather than from cells in the EZ, at a distance from the lesion (Buffo et al., 2008; Cavanagh, 1970; Chen et al., 2008). Several studies have described the ability of adult parenchymal astrocytes to adopt a multipotent stem cell-like phenotype after injury (Buffo et al., 2008; Steindler and Laywell, 2003). However, we found no evidence of astrocyte multipotency after spinal cord demyelination because *Fgfr3*$^+$ cells gave rise only to AQP4$^+$ astrocytes but not to oligodendrocytes or Schwann cells. We found no evidence of neurogenesis during the repair of lysolecithin lesions, in contrast to reports suggesting generation of white matter neurons after immune-mediated injury to spinal cord white matter (Danilov et al., 2006).

In summary, we have used a genetic fate mapping approach to show that, during the reconstruction of demyelinating lesions in adult white matter, new remyelinating oligodendrocytes and Schwann cells are mainly derived from adult OLPs whereas new astrocytes are derived mainly from other astrocytes. Our results together with those of others provide evidence that adult OLPs/NG2 cells have a wider differentiation potential than previously thought, exhibiting the capacity to differentiate into Schwann cells of neural crest lineage as well as all three neuroepithelial lineages (neurons, astrocytes, and oligodendrocytes) (Belachew et al., 2003; Dimou et al., 2008; Kondo and Raff, 2000; Nunes et al., 2003; Rivers et al., 2008). A definitive demonstration of adult OLP multipotency would require clonally derived cells. However, clonal derivation from single adult OLPs is not technically feasible at present. Future studies are likely to focus on a more detailed analysis of how and why CNS precursor/stem cells give rise to Schwann cells and—critically important from a translational perspective—whether repair of demyelinated lesions by CNS-derived oligodendrocytes or Schwann cells is preferable.

EXPERIMENTAL PROCEDURES

Animals

Pdgfra-creER^{T2}, *Fgfr3-icreER*^{T2} and *P*$_0$*-creER*^{T2} transgenic mice have been described (Leone et al., 2003; Rivers et al., 2008; Young et al., 2010). *Olig2-cre* mice were produced via blastocyst injection of ESCs in which an *IRES-Cre-lox-PGK-Neo-lox* cassette was introduced into the single exon of *Olig2* and *PGK-Neo* subsequently removed with Cre (D.H.R., N.K., and W.D.R., unpublished). Mice were housed under standard laboratory conditions on a 12 hr light/dark cycle with constant access to food and water. Homozygous or heterozygous Cre mice were crossed with homozygous *Rosa26-YFP* reporters to generate double-heterozygous offspring for analysis. Demyelination experiments were performed on female mice aged 11–13 weeks (nominally post-natal day 85, P85) according to the principles of laboratory animal care approved by the UK Home Office. Requests for mice

from the Richardson laboratory can be made via http://www.ucl.ac.uk/~ucbzwdr/Richardson.htm.

Tamoxifen Induction

Cre recombination was induced by administering tamoxifen (Sigma, 40 mg/ml), dissolved in corn oil by sonication for 45 min at 30°C. Adult mice were given 300 mg per kg of body weight by oral gavage on 4 consecutive days, then allowed to recover for 4 days prior to inducing demyelination on ~P85. In spinal cords of *Pdgfra-creER^{T2}: Rosa26-YFP* mice examined 1 day after the final dose of tamoxifen, 39% ± 7% of PDGFRA^{+} OLPs were labeled for YFP (mean ± SEM; n = 5). In *Fgfr3-icreER^{T2}*: *Rosa26-YFP* mice subjected to a similar regimen, practically all ependymal cells of the central canal and a high proportion (>95%) of *Fgfr3*-expressing astrocytes in the parenchyma labeled for YFP (Rivers et al., 2008 and not shown). The *Olig2-cre* line drove Cre recombination in all oligodendrocyte-lineage cells and motor neurons (Kessaris et al., 2006). In *P_0-creER^{T2}* mice, 83% ± 2% of cells in the ventral and dorsal roots became YFP labeled.

Surgical Procedures

Four days after tamoxifen induction, mice underwent a spinal cord white matter demyelination. In brief, mice received subcutaneous buprenorphine (30 μg per kg of body weight) as analgesic treatment and were anesthetized with isoflurane. Demyelination was induced by injection of 1 μl of 1% Lα-lysophosphatidylcholine (lysolecithin, SIGMA) or 0.1% ethidium bromide (EB) into the ventral or dorsal white matter funiculus at the level of T12 as previously described in detail (Arnett et al., 2004). The position of T13 was identified and the epaxial musculature was cleared from the immediate area. The space between T12 and T13 was exposed and carefully cleared, the central vein was identified, and the dura was pierced with a dental needle lateral to the vein. A three-way manipulator was then used to position the needle for stereotaxic injection of lysolecithin or EB. Hamilton needle with a fine glass tip was advanced through the pierced dura at an angle appropriate for ventrolateral or dorsal funiculus injection. Injection was controlled at 1 ml per minute and the needle remained in the injection site for 2 min to allow maximal diffusion of toxin. For sciatic nerve crush, an incision was made over the length of the right hip and, after exposing the sciatic nerve, haemostatic forceps were used for 45 s to induce a crush injury of the sciatic nerve. Lesions in adult rat cerebellar peduncle and spinal cord were as previously described (Shields et al., 1999; Woodruff and Franklin, 1999).

Tissue Preparation

Mice were anesthetized with pentobarbitone and perfused through the ascending aorta with 4% (w/v) paraformaldehyde (PFA, Sigma) in phosphate-buffered saline (PBS) (pH 7.4). Unfixed tissue was used for reverse transcriptase-PCR. The tissue surrounding the injection site was dissected, postfixed in 4% PFA at 4°C overnight, cryo-preserved in 30% (w/v) sucrose for 12–24 hr at 4°C, embedded in OCT, frozen on dry ice, and sectioned in a cryotome (12 μm). Coronal and longitudinal cryo-sections were thaw-mounted onto Poly-L-lysine-coated slides and stored at −80°C.

Immunohistochemistry

Frozen sections, after several rinses in PBS, were permeabilized and blocked with PBS containing 0.3% (v/v)Triton X-100 and 10% (v/v) donkey serum in PBS for 1 hr at room temperature (RT, 20-25°C), then incubated for 12 hr at 4°C with primary antibodies followed by incubation with fluorophore-conjugated secondary antibodies for 1 hr at RT. Primary and secondary antibodies were diluted in PBS containing 0.1% Triton X-100. For double or triple labeling, the above procedure was repeated sequentially with primary

antibodies from different animal species and distinguishable fluorophore-conjugated secondary antibodies. Slides were coverslipped in mounting medium containing DAPI dye (Dako) and examined under the fluorescence microscope. The following primary antibodies were used: PDGFRA (rat, 1:500, BD Sciences), GFP (rabbit, 1:6000, goat, 1:2000, chicken, 1:2000, AbCam), NG2 (rabbit, 1:500, Chemicon), OLIG2 (rabbit serum, 1:6000, from Dr. Charles Stiles, Dana-Farber Cancer Institute, Boston, MA), GFAP (rabbit, 1:1000, Dako), S100 (rabbit, 1:100, Dako), DCX (rabbit, 1:1000, AbCam), AQP4 (rabbit, 1:1000, AbCam), SMI31 (mouse, 1:400, Sternberger), Periaxin (rabbit, 1:3000, from Peter Brophy, Centre for Neuroscience Research, University of Edinburgh, UK), P75 (rabbit, 1:1000, SIGMA), OCT6 (rabbit, 1:4000, from Dr. John Bermingham Jr., McLaughlin Research Institute, Great Falls, MT), Transferrin (rabbit, 1:1000, AbCam), CC1 (mouse, 1:200, Calbiochem), Fibronectin (rabbit, 1:500, Millipore). Secondary antibodies were: Alexa Fluor 488-, 568-, or 647-conjugated donkey antibodies against mouse, rat rabbit, or goat IgG or IgG1 (1:1000, all from Invitrogen). In situ hybridization with *Pdgfa* and P_0 riboprobes and the combination of in situ hybridization with immunohistochemistry was as previously described (Fancy et al., 2004; Sim et al., 2002a).

Dye-Filling Live Cells

To dye-fill live cells we prepared 300 μm live brain slices of tamoxifen-induced *Pdgfra-creER^{T2}/Rosa26-YFP* mice via a vibratome. YFP$^+$ cell bodies were visible in the two-photon laser scanning microscope at a 890 nm excitation wavelength. Positive cells were filled with 20 μM Alexa Fluor 488 dye through a 9–12 MΩ glass pipette. Images of cells before and after filling were collected with custom-made ScanImage software and analyzed with ImageJ software (http://rsbweb.nih.gov.gate1.inist.fr/ij/).

Semiquantitative RT-PCR

Total RNA was isolated from freshly isolated sciatic nerve samples and OLP cultures via Trizol reagent, cleaned with RNeasy Mini kit (QIAGEN), and treated with DNase I prior to cDNA synthesis. One microgram of total RNA was reversed transcribed into cDNA with oligo-$(dT)_{12–18}$ primers and Sensiscript Reverse Transcriptase according to the manufacturer's recommendations (Invitrogen). Two microliters of cDNA were amplified in a thermal cycler with the following program for each primer pairs: denaturation at 95°C for 45 s, annealing at a primer-specific temperature for 45 s, followed by extension at 72°C for 1 min, for 40 cycles to enhance the signal. The sequences of the PCR primers used (5′-3′) were: *Olig2* forward ttccagaacctggttgactc, reverse ttgggattattccattcca; *Pdgfra* forward ggtcccatttacatcatcac, reverse attcctcga gcaacttgata; *Cyclophilin* (a control housekeeping gene) forward tgagcactggg gagaaag, reverse aggggaatgaggaaaatatgg.

Microscopy

For cell imaging and counting, micrographs were acquired with a 203 objective on a Zeiss Axioplan fluorescent microscope under an appropriate filter with a digital camera. Composite images were assembled with Adobe Photoshop and defined areas were measured with Carl Zeiss AxioVision 4.5. The lesion area was defined by the density of DAPI-stained nuclei present in the injured white matter, a feature of inflammatory response to demyelination, or by solochrome cyanine staining on adjacent sections to those used for immunohistochemistry. Sections from at least five mice were analyzed for each data point. A Leica SP2 confocal laser scanning microscope with Leica Lite software was used for most of the micrography. The optical slice thickness was 0.5–1 μm. Images were processed with Image J (NIH) software.

Supplementary Material

Refer to Web version on PubMed Central for supplementary material.

Acknowledgments

M.Z. was supported by a Marie Curie Fellowship from the European Union (EU). L.E.R. was supported by a studentship from the Biotechnology and Biological Sciences Research Council with Eisai Research London, M.R. by a Wellcome Trust Prize Studentship, and F.J. by an EU Marie Curie Fellowship. D.H.R. is an HHMI investigator. U.S. is supported by the Swiss National Science Foundation and the National Competence Center in Research (NCCR) “Neural Plasticity and Repair.” N.K. and W.D.R. are funded by the UK Medical Research Council and The Wellcome Trust. S.P.J.F., C.Z., and R.J.M.F. are supported by grants from the UK MS Society and the National MS Society.

REFERENCES

Arnett HA, Fancy SPJ, Alberta JA, Zhao C, Plant SR, Kaing S, Raine CS, Rowitch DH, Franklin RJ, Stiles CD. bHLH transcription factor Olig1 is required to repair demyelinated lesions in the CNS. Science. 2004; 306:2111–2115. [PubMed: 15604411]

Baron-Van Evercooren A, Avellana-Adalid V, Ben Younes-Chennoufi A, Gansmuller A, Nait-Oumesmar B, Vignais L. Cell-cell interactions during the migration of myelin-forming cells transplanted in the demyelinated spinal cord. Glia. 1996; 16:147–164. [PubMed: 8929902]

Belachew S, Chittajallu R, Aguirre AA, Yuan X, Kirby M, Anderson S, Gallo V. Postnatal NG2 proteoglycan-expressing progenitor cells are intrinsically multipotent and generate functional neurons. J. Cell Biol. 2003; 161:169–186. [PubMed: 12682089]

Blakemore WF. Remyelination by Schwann cells of axons demyelinated by intraspinal injection of 6-aminonicotinamide in the rat. J. Neurocytol. 1975; 4:745–757. [PubMed: 127832]

Blakemore WF, Franklin RJM. Remyelination in experimental models of toxin-induced demyelination. Curr. Top. Microbiol. Immunol. 2008; 318:193–212. [PubMed: 18219819]

Buffo A, Rite I, Tripathi P, Lepier A, Colak D, Horn AP, Mori T, Götz M. Origin and progeny of reactive gliosis: A source of multipotent cells in the injured brain. Proc. Natl. Acad. Sci. USA. 2008; 105:3581–3586. [PubMed: 18299565]

Cassiani-Ingoni R, Coksaygan T, Xue H, Reichert-Scrivner SA, Wiendl H, Rao MS, Magnus T. Cytoplasmic translocation of Olig2 in adult glial progenitors marks the generation of reactive astrocytes following autoimmune inflammation. Exp. Neurol. 2006; 201:349–358. [PubMed: 16814281]

Cavanagh JB. The proliferation of astrocytes around a needle wound in the rat brain. J. Anat. 1970; 106:471–487. [PubMed: 4912665]

Chandran S, Compston A, Jauniaux E, Gilson J, Blakemore W, Svendsen C. Differential generation of oligodendrocytes from human and rodent embryonic spinal cord neural precursors. Glia. 2004; 47:314–324. [PubMed: 15293229]

Chen Y, Miles DK, Hoang T, Shi J, Hurlock E, Kernie SG, Lu QR. The basic helix-loop-helix transcription factor olig2 is critical for reactive astrocyte proliferation after cortical injury. J. Neurosci. 2008; 28:10983–10989. [PubMed: 18945906]

Crang AJ, Gilson JM, Li WW, Blakemore WF. The remyelinating potential and in vitro differentiation of MOG-expressing oligodendrocyte precursors isolated from the adult rat CNS. Eur. J. Neurosci. 2004; 20:1445–1460. [PubMed: 15355312]

Danilov AI, Covacu R, Moe MC, Langmoen IA, Johansson CB, Olsson T, Brundin L. Neurogenesis in the adult spinal cord in an experimental model of multiple sclerosis. Eur. J. Neurosci. 2006; 23:394–400. [PubMed: 16420447]

Dimou L, Simon C, Kirchhoff F, Takebayashi H, Götz M. Progeny of Olig2-expressing progenitors in the gray and white matter of the adult mouse cerebral cortex. J. Neurosci. 2008; 28:10434–10442. [PubMed: 18842903]

Duncan ID, Hoffman RL. Schwann cell invasion of the central nervous system of the myelin mutants. J. Anat. 1997; 190:35–49. [PubMed: 9034880]

Dusart I, Marty S, Peschanski M. Demyelination and remyelination by Schwann cells and oligodendrocytes after kainate-induced neuronal depletion in the central nervous system. Neuroscience. 1992; 5:137–148. [PubMed: 1465177]

Fancy SPJ, Zhao C, Franklin RJM. Increased expression of Nkx2.2 and Olig2 identifies reactive oligodendrocyte progenitor cells responding to demyelination in the adult CNS. Mol. Cell. Neurosci. 2004; 27:247–254. [PubMed: 15519240]

Felts PA, Woolston AM, Fernando HB, Asquith S, Gregson NA, Mizzi OJ, Smith KJ. Inflammation and primary demyelination induced by the intraspinal injection of lipopolysaccharide. Brain. 2005; 128:1649–1666. [PubMed: 15872019]

Franklin RJM, Blakemore WF. Requirements for Schwann cell migration within CNS environments: A viewpoint. Int. J. Dev. Neurosci. 1993; 11:641–649. [PubMed: 8116476]

Franklin RJM, ffrench-Constant C. Remyelination in the CNS: From biology to therapy. Nat. Rev. Neurosci. 2008; 9:839–855. [PubMed: 18931697]

Gensert JM, Goldman JE. Endogenous progenitors remyelinate demyelinated axons in the adult CNS. Neuron. 1997; 19:197–203. [PubMed: 9247275]

Gillespie CS, Sherman DL, Blair GE, Brophy PJ. Periaxin, a novel protein of myelinating Schwann cells with a possible role in axonal ensheathment. Neuron. 1994; 12:497–508. [PubMed: 8155317]

Gudiño-Cabrera G, Nieto-Sampedro M. Schwann-like macroglia in adult rat brain. Glia. 2000; 30:49–63. [PubMed: 10696144]

Itoyama Y, Webster HD, Richardson EP Jr. Trapp BD. Schwann cell remyelination of demyelinated axons in spinal cord multiple sclerosis lesions. Ann. Neurol. 1983; 14:339–346. [PubMed: 6195956]

Itoyama Y, Ohnishi A, Tateishi J, Kuroiwa Y, Webster HD. Spinal cord multiple sclerosis lesions in Japanese patients: Schwann cell remyelination occurs in areas that lack glial fibrillary acidic protein (GFAP). Acta Neuropathol. 1985; 65:217–223. [PubMed: 2579518]

Keirstead HS, Blakemore WF. Identification of post-mitotic oligodendrocytes incapable of remyelination within the demyelinated adult spinal cord. J. Neuropathol. Exp. Neurol. 1997; 56:1191–1201. [PubMed: 9370229]

Keirstead HS, Ben-Hur T, Rogister B, O'Leary MT, Dubois-Dalcq M, Blakemore WF. Polysialylated neural cell adhesion molecule-positive CNS precursors generate both oligodendrocytes and Schwann cells to remyelinate the CNS after transplantation. J. Neurosci. 1999; 19:7529–7536. [PubMed: 10460259]

Kessaris N, Fogarty M, Iannarelli P, Grist M, Wegner M, Richardson WD. Competing waves of oligodendrocytes in the forebrain and post-natal elimination of an embryonic lineage. Nat. Neurosci. 2006; 9:173–179. [PubMed: 16388308]

Kondo T, Raff M. Oligodendrocyte precursor cells reprogrammed to become multipotential CNS stem cells. Science. 2000; 289:1754–1757. [PubMed: 10976069]

Kondo T, Raff MC. A role for Noggin in the development of oligodendrocyte precursor cells. Dev. Biol. 2004; 267:242–251. [PubMed: 14975730]

Lee MJ, Brennan A, Blanchard A, Zoidl G, Dong Z, Tabernero A, Zoidl C, Dent MAR, Jessen KR, Mirsky R. P0 is constitutively expressed in the rat neural crest and embryonic nerves and is negatively and positively regulated by axons to generate non-myelin-forming and myelin-forming Schwann cells, respectively. Mol. Cell. Neurosci. 1997; 8:336–350. [PubMed: 9073396]

Leone DP, Genoud S, Atanasoski S, Grausenburger R, Berger P, Metzger D, Macklin WB, Chambon P, Suter U. Tamoxifeninducible glia-specific Cre mice for somatic mutagenesis in oligodendrocytes and Schwann cells. Mol. Cell. Neurosci. 2003; 22:430–440. [PubMed: 12727441]

Levison SW, Goldman JE. Both oligodendrocytes and astrocytes develop from progenitors in the subventricular zone of postnatal rat forebrain. Neuron. 1993; 10:201–212. [PubMed: 8439409]

Ligon KL, Kesari S, Kitada M, Sun T, Arnett HA, Alberta JA, Anderson DJ, Stiles CD, Rowitch DH. Development of NG2 neural progenitor cells requires Olig gene function. Proc. Natl. Acad. Sci. USA. 2006; 103:7853–7858. [PubMed: 16682644]

Magnus T, Coksaygan T, Korn T, Xue H, Arumugam TV, Mughal MR, Eckley DM, Tang SC, Detolla L, Rao MS, et al. Evidence that nucleocytoplasmic Olig2 translocation mediates brain-injury-

induced differentiation of glial precursors to astrocytes. J. Neurosci. Res. 2007; 85:2126–2137. [PubMed: 17510983]

Masahira N, Takebayashi H, Ono K, Watanabe K, Ding L, Furusho M, Ogawa Y, Nabeshima Y, Alvarez-Buylla A, Shimizu K, Ikenaka K. Olig2-positive progenitors in the embryonic spinal cord give rise not only to motoneurons and oligodendrocytes, but also to a subset of astrocytes and ependymal cells. Dev. Biol. 2006; 293:358–369. [PubMed: 16581057]

Mujtaba T, Mayer-Proschel M, Rao MS. A common neural progenitor for the CNS and PNS. Dev. Biol. 1998; 200:1–15. [PubMed: 9698451]

Nagelhus EA, Veruki ML, Torp R, Haug FM, Laake JH, Nielsen S, Agre P, Ottersen OP. Aquaporin-4 water channel protein in the rat retina and optic nerve: Polarized expression in Müller cells and fibrous astrocytes. J. Neurosci. 1998; 18:2506–2519. [PubMed: 9502811]

Nave KA, Trapp BD. Axon-glial signaling and the glial support of axon function. Annu. Rev. Neurosci. 2008; 31:535–561. [PubMed: 18558866]

Nishiyama A, Lin XH, Giese N, Heldin CH, Stallcup WB. Co-localization of NG2 proteoglycan and PDGF alpha-receptor on O2A progenitor cells in the developing rat brain. J. Neurosci. Res. 1996; 43:299–314. [PubMed: 8714519]

Nunes MC, Roy NS, Keyoung HM, Goodman RR, McKhann G 2nd, Jiang L, Kang J, Nedergaard M, Goldman SA. Identification and isolation of multipotential neural progenitor cells from the subcortical white matter of the adult human brain. Nat. Med. 2003; 9:439–447. [PubMed: 12627226]

Patrikios P, Stadelmann C, Kutzelnigg A, Rauschka H, Schmidbauer M, Laursen H, Sorensen PS, Brück W, Lucchinetti C, Lassmann H. Remyelination is extensive in a subset of multiple sclerosis patients. Brain. 2006; 129:3165–3172. [PubMed: 16921173]

Pringle NP, Mudhar HS, Collarini EJ, Richardson WD. PDGF receptors in the rat CNS: during late neurogenesis, PDGF alpha-receptor expression appears to be restricted to glial cells of the oligodendrocyte lineage. Development. 1992; 115:535–551. [PubMed: 1425339]

Raff MC, Miller RH, Noble M. A glial progenitor cell that develops in vitro into an astrocyte or an oligodendrocyte depending on culture medium. Nature. 1983; 303:390–396. [PubMed: 6304520]

Raivich G, Kreutzberg GW. Expression of growth factor receptors in injured nervous tissue. II. Induction of specific platelet-derived growth factor binding in the injured PNS is associated with a breakdown in the blood-nerve barrier and endoneurial interstitial oedema. J. Neurocytol. 1987; 16:701–711. [PubMed: 2826710]

Rivers LE, Young KM, Rizzi M, Jamen F, Psachoulia K, Wade A, Kessaris N, Richardson WD. PDGFRA/NG2 glia generate myelinating oligodendrocytes and piriform projection neurons in adult mice. Nat. Neurosci. 2008; 11:1392–1401. [PubMed: 18849983]

Shields SA, Gilson JM, Blakemore WF, Franklin RJM. Remyelination occurs as extensively but more slowly in old rats compared to young rats following gliotoxin-induced CNS demyelination. Glia. 1999; 28:77–83. [PubMed: 10498825]

Sim FJ, Zhao C, Li WW, Lakatos A, Franklin RJM. Expression of the POU-domain transcription factors SCIP/Oct-6 and Brn-2 is associated with Schwann cell but not oligodendrocyte remyelination of the CNS. Mol. Cell. Neurosci. 2002a; 20:669–682. [PubMed: 12213447]

Sim FJ, Zhao C, Penderis J, Franklin RJM. The age-related decrease in CNS remyelination efficiency is attributable to an impairment of both oligodendrocyte progenitor recruitment and differentiation. J. Neurosci. 2002b; 22:2451–2459. [PubMed: 11923409]

Smith EJ, Blakemore WF, McDonald WI. Central remyelination restores secure conduction. Nature. 1979; 280:395–396. [PubMed: 460414]

Snyder DH, Valsamis MP, Stone SH, Raine CS. Progressive demyelination and reparative phenomena in chronic experimental allergic encephalomyelitis. J. Neuropathol. Exp. Neurol. 1975; 34:209–221. [PubMed: 1141960]

Steindler DA, Laywell ED. Astrocytes as stem cells: Nomenclature, phenotype, and translation. Glia. 2003; 43:62–69. [PubMed: 12761868]

Talbott JF, Loy DN, Liu Y, Qiu MS, Bunge MB, Rao MS, Whittemore SR. Endogenous Nkx2.2+/Olig2+ oligodendrocyte precursor cells fail to remyelinate the demyelinated adult rat spinal cord in the absence of astrocytes. Exp. Neurol. 2005; 192:11–24. [PubMed: 15698615]

Talbott JF, Cao Q, Enzmann GU, Benton RL, Achim V, Cheng XX, Mills MD, Rao MS, Whittemore SR. Schwann cell-like differentiation by adult oligodendrocyte precursor cells following engraftment into the demyelinated spinal cord is BMP-dependent. Glia. 2006; 54:147–159. [PubMed: 16921543]

Trapp BD, Nave KA. Multiple sclerosis: An immune or neurode-generative disorder? Annu. Rev. Neurosci. 2008; 31:247–269. [PubMed: 18558855]

Watanabe M, Toyama Y, Nishiyama A. Differentiation of proliferated NG2-positive glial progenitor cells in a remyelinating lesion. J. Neurosci. Res. 2002; 69:826–836. [PubMed: 12205676]

Woodruff RH, Franklin RJM. Demyelination and remyelination of the caudal cerebellar peduncle of adult rats following stereotaxic injections of lysolecithin, ethidium bromide, and complement/anti-galactocerebroside: A comparative study. Glia. 1999; 25:216–228. [PubMed: 9932868]

Young KM, Mitsumori T, Pringle N, Grist M, Kessaris N, Richardson WD. An Fgfr3-iCreER(T2) transgenic mouse line for studies of neural stem cells and astrocytes. Glia. 2010 in press. Published online February 12, 2010.

Zhang SC, Ge B, Duncan ID. Adult brain retains the potential to generate oligodendroglial progenitors with extensive myelination capacity. Proc. Natl. Acad. Sci. USA. 1999; 96:4089–4094. [PubMed: 10097168]

Zhu X, Bergles DE, Nishiyama A. NG2 cells generate both oligodendrocytes and gray matter astrocytes. Development. 2008; 135:145–157. [PubMed: 18045844]

Europe PMC Funders Author Manuscripts

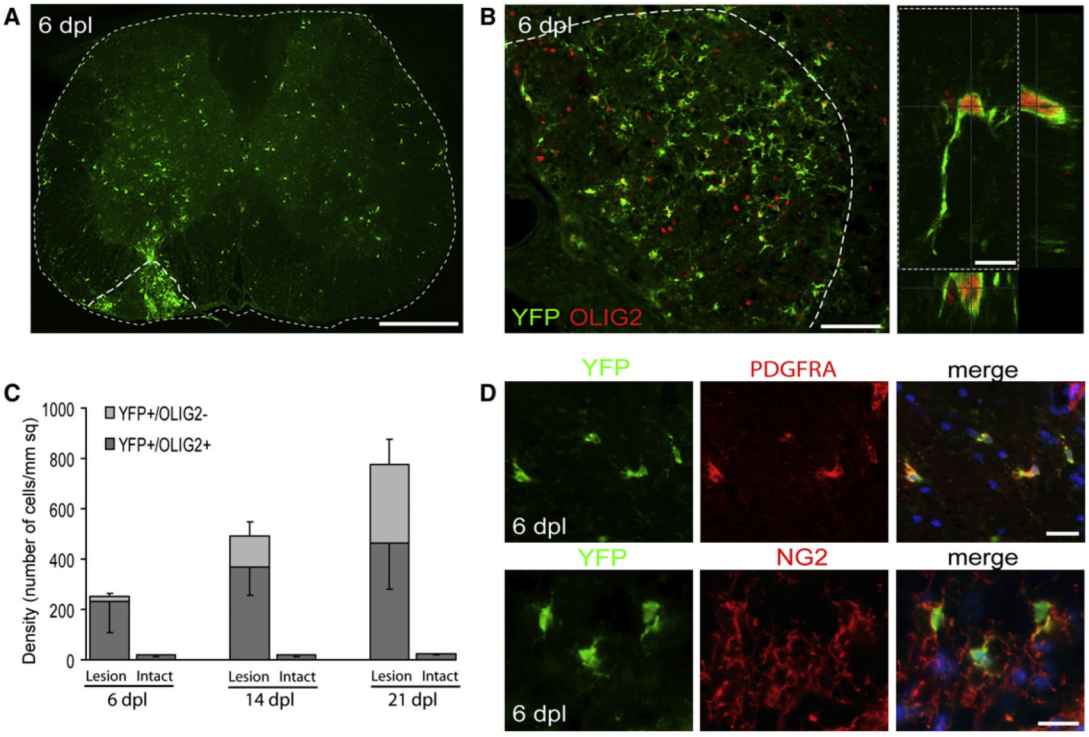

Figure 1. Identification of Genetically Labeled PDGFRA$^+$ Cells in the Intact and Demyelinated Adult Spinal Cord

(A) Six days after induction of demyelination by injection of lysolecithin into the left ventrolateral white matter (dotted line), YFP$^+$ cells can be seen throughout the white and gray matter and particularly concentrated within the lesion area (dpl, days postlesion; scale bar represents 500 μm).

(B) Many of the YFP$^+$ cells express OLIG2 in their nuclei (scale bars represent 100 μm in low-power image and 10 μm in higher-magnification confocal image).

(C) Density of YFP$^+$/OLIG2$^-$ and YFP$^+$/OLIG2$^+$ cells in normal nondemyelinated (intact) and demyelinated (lesion) tissue at 6, 14, and 21 DPL (n = 7, mean ± SD).

(D) Nearly all YFP$^+$ cells coexpress the OLP markers NG2 and PDGFRA (scale bars represent 20 μm).

Europe PMC Funders Author Manuscripts

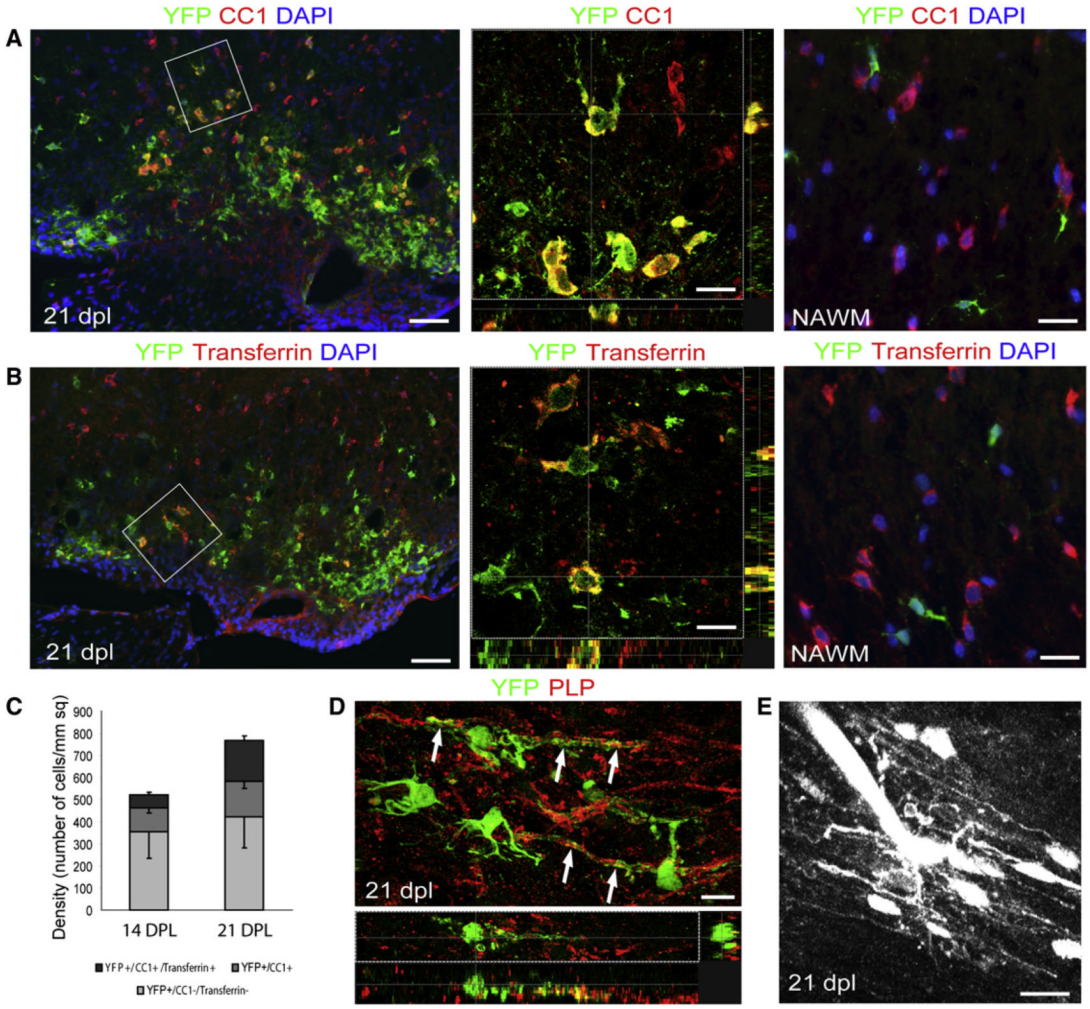

Figure 2. Expression of Mature Oligodendrocyte Markers in YFP$^+$ Cells with Morphological Features of Myelinating Oligodendrocytes

(A and B) Confocal images of spinal cord cross sections at 21 dpl immunostained with (A) anti-CC1 and (B) anti-Transferrin antibodies (scale bar represent 45 μm). High-power confocal projections of z-stacks show double-labeled cells from boxed regions (scale bars represent 10 μm). In the normal appearing white matter (NAWM), YFP$^+$ cells do not express mature oligodendrocyte markers (scale bar, 20 μm).

(C) Density of YFP$^+$ cells expressing CC1 alone or CC1 and Transferrin at 14 and 21 dpl.

(D) Longitudinal section of a remyelinated area at 21 dpl showing YPF$^+$ processes closely associated with PLP$^+$ myelin sheaths (arrows, scale bar represents 10 μm).

(E) Alexa dye labeling of a YFP$^+$ cell at 21 dpl by electroporation reveals a cell with a distinctive multiprocessed morphology characteristic of a myelinating oligodendrocyte (scale bar represents 20 μm, see also Movie S1).

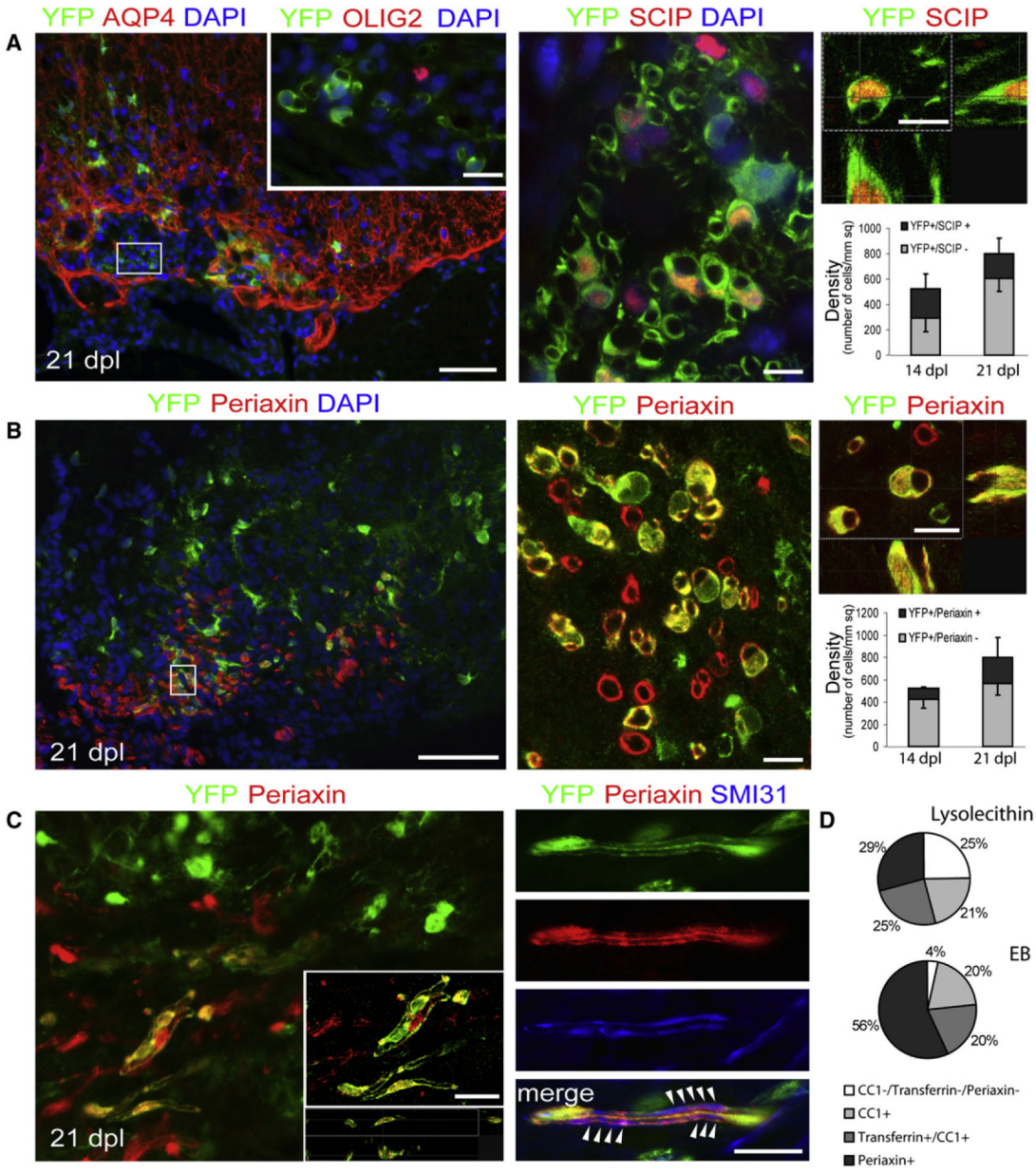

Figure 3. *Pdgfa-creER^{T2}* Cells Give Rise to Myelinating Schwann Cells

(A) At 21 dpl, AQP-4 immunonegative (astrocyte-free) areas of the lesions can be identified containing YFP$^+$/OLIG2-negative cells with morphologies resembling myelinating Schwann cells (left image) (the inset shows a group of cells in an adjacent section [corresponding to the boxed area], immunolabeled for OLIG2). Scale bars represent 100 μm (left image) and 20 μm (inset). Many of these YFP$^+$ cells express the Schwann cell transcription factor SCIP within their nuclei (middle and right images, scale bar represents 10 μm). The histograms show the density of YFP$^+$/SCIP$^-$ and YFP$^+$/SCIP$^+$ cells at 14 and 21 dpl.

(B) YFP$^+$ cells with Schwann cell-like morphology are associated with Periaxin$^+$ myelin sheaths (scale bar represents 50 μm). The boxed area in the left panel is shown at higher magnification in the middle panel and as a confocal Z-projection in the top right panel (scale

bar represents 10 μm). The histograms show the density of YFP^+/$Periaxin^-$ and YFP^+/$Periaxin^+$ cells at 14 and 21 dpl.
(C) $Periaxin^+$ cells derived from $PDGFRA^+$ precursors at 21 days after lesion show 1:1 interactions with two parallel $SMI31^+$ axons in longitudinal section (indicated by arrowheads on merged image; scale bars represent 20 μm).
(D) During remyelination of EB-induced lesions, a higher percentage of YFP^+ cells coexpressed $Periaxin^+$ than in lysolecithin-induced lesions at 21 dpl, while the proportion of remyelinating oligodendrocytes generated from $PDGFRA^+$ precursors is approximately the same for both lesion types ($p > 0.5$, data expressed as percentage of YFP^+ cells ± SEM).

Europe PMC Funders Author Manuscripts

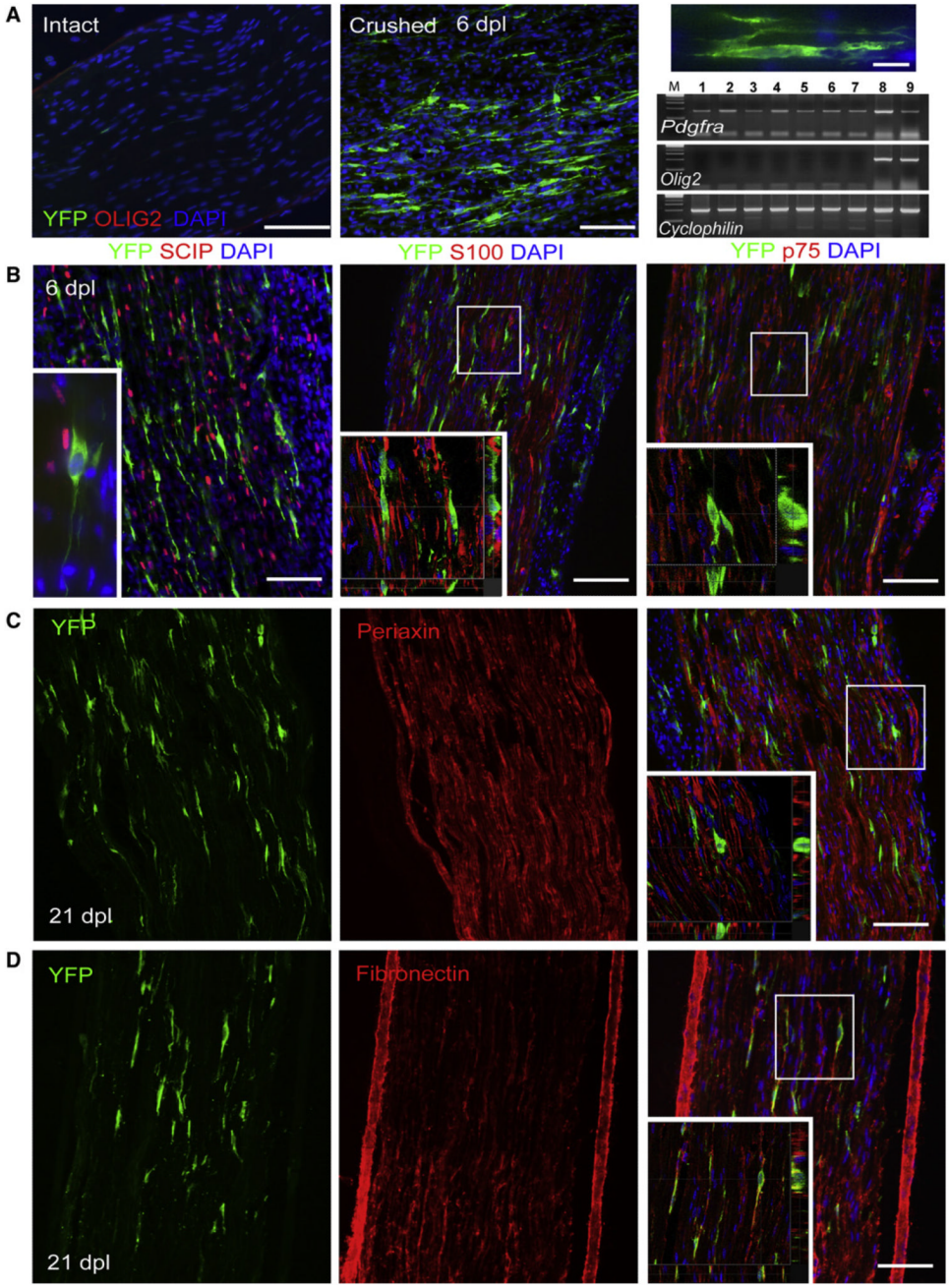

Figure 4. PDGFRA Expression in Intact and Injured Sciatic Nerve of *Pdgfra-creER*^{T2} Mice

(A) YFP^{+} cells are detected at 6 days after nerve crush but not in intact noncrushed nerve; OLIG2 is not detected in either intact or crushed nerves. Longitudinal sections of sciatic nerves were double immuno-labeled for YFP and OLIG2 (scale bars represent 100 μm and 20 μm in low- and high-magnification images, respectively). RT-PCR analysis confirmed the lack of *Olig2* transcripts in the intact or crushed sciatic nerve (lane 1, control intact nerve; lane 2, crushed nerve, 6 hr; lane 3, intact nerve, 24 hr; lane 4, crushed, 24 hr; lane 5, intact, 6 dpl; lane 6, crushed, 6 dpl; lane 7, dorsal root ganglia; compared with the level of expression in cultured OLPs; lanes 8 and 9, RNA from two separate OLP cultures), while

Pdgfra can be detected in both intact and injured nerve (a housekeeping gene, *Cyclophilin*, was used as a normalization control).
(B) Immunohistochemical characterization of YFP-expressing cells in 6 dpl sciatic nerve. YFP^+ cells do not coexpress early Schwann cell markers such as SCIP, S100, and p75. Micrographs of longitudinal sections stained with anti-YFP and Schwann cell markers (main image scale bars represent 100 μm) and higher-magnification confocal projections of two different optical sections from the same field show nonoverlap between YFP and Schwann cell markers on any z-levels (inset scale bar represents 30 μm).
(C and D) At 21 dpl some YFP^+ cells could still be detected which strongly expressed fibronectin (D) but did not express Periaxin (C).

Europe PMC Funders Author Manuscripts

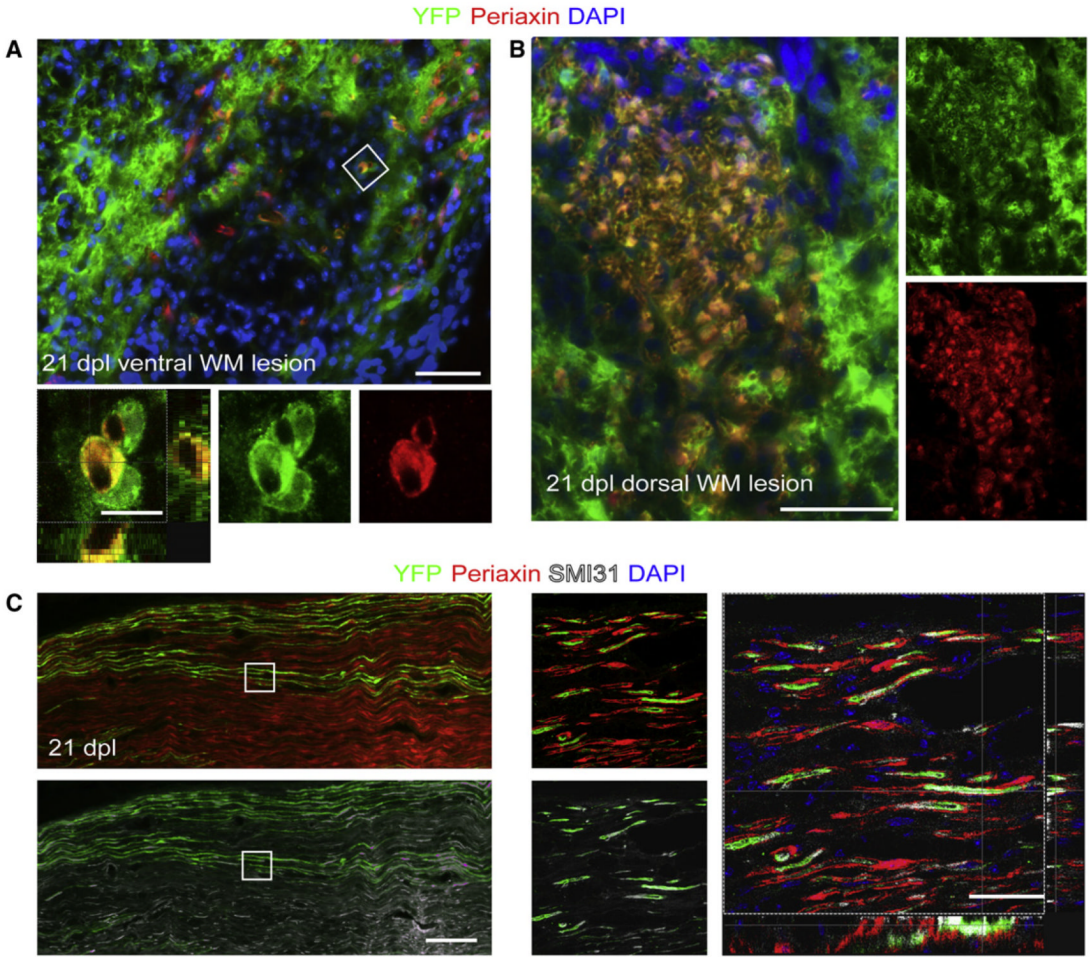

Figure 5. Remyelinating Schwann cells within CNS Lesion Derived from *Olig2*$^+$ Cells

(A) Immunostaining for YFP and Periaxin performed on spinal cord cross sections from *Olig2-cre: Rosa26-YFP* mice at 21 days after lysolecithin-induced demyelination in ventral spinal cord white matter reveals cells expressing both markers (scale bar represents 50 μm) (confocal projection of cells from the boxed area, lower panel, scale bar represents 10 μm).

(B) Overlay confocal image showing a high level of YFP/Periaxin colocalization (single channels for YFP and Periaxin; scale bar represents 50 μm) confirming that nearly all of Periaxin$^+$ cells remyelinating lesions in the dorsal funiculus are generated from *Olig2-cre*-expressing cells.

(C) YFP was expressed within sciatic nerve axons in *Olig2-cre:Rosa26-YFP* mice. There were no YFP$^+$ cell bodies detected in injured sciatic nerves 28 days after nerve crush. Micrographs and confocal projections of longitudinal sections through the nerve show colocalization of YFP and SMI31 (axonal marker) but no overlap of YFP with the Schwann cell myelin protein Periaxin (scale bars represent 20 μm).

Europe PMC Funders Author Manuscripts

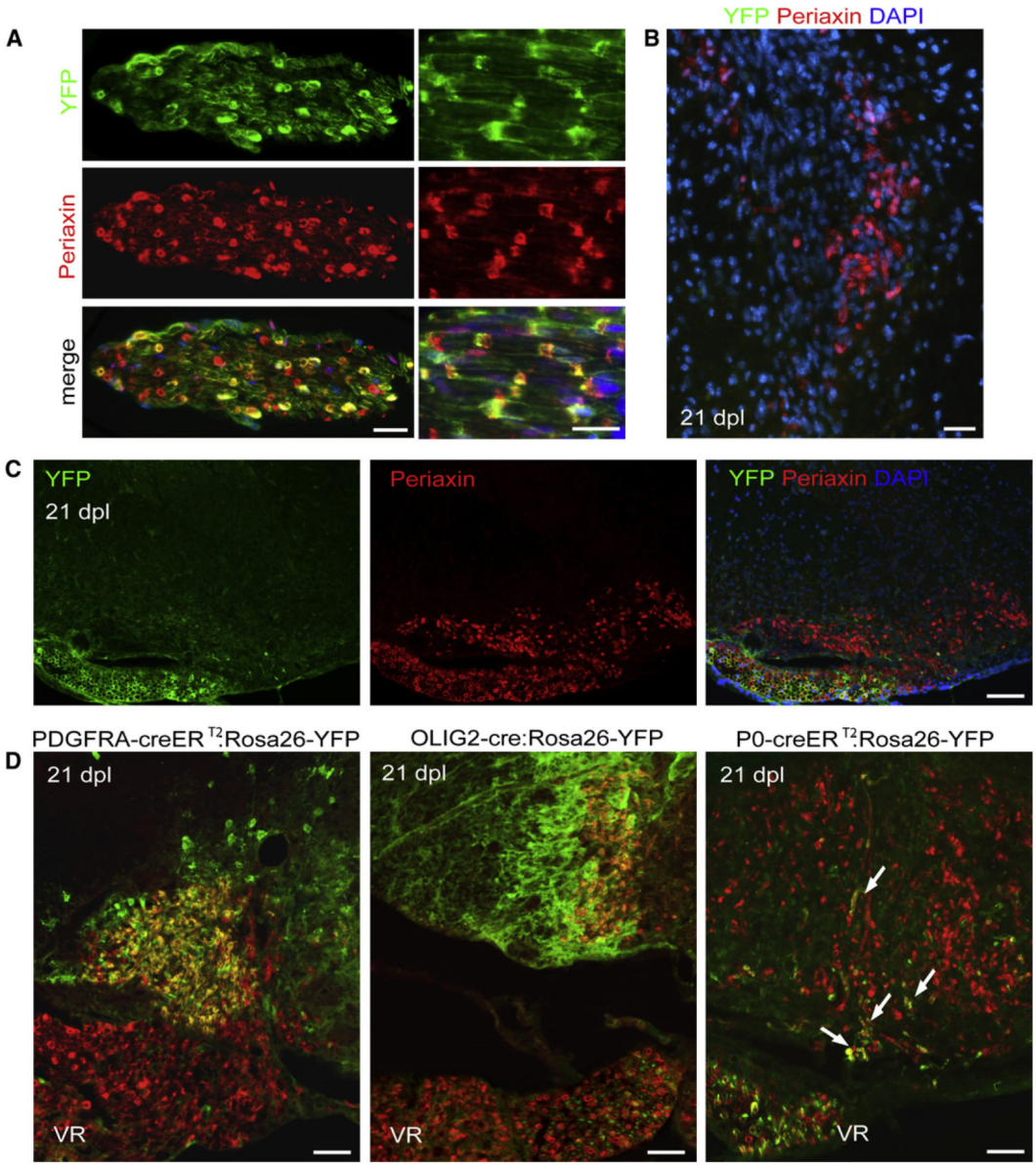

Figure 6. Some Periaxin$^+$ Cells within Remyelinating CNS Lesions Are Derived from P_0-Expressing Cells of the PNS, whereas the Majority Is Derived from PDGFRA- and OLIG2-Expressing CNS-Derived Cells

(A) Longitudinal and transverse sections of ventral root from *P_0-creER^{T2}:Rosa26-YFP* mice stained with anti-YFP and anti-Periaxin antibody show high efficiency of recombination 83% ± 2% (scale bars represent 30 μm).

(B) No Periaxin$^+$ cells generated from *P_0-creER^{T2}*-expressing cells are detected in the dorsal lysolecithin-induced lesions at 21 dpl (scale bars represent 30 μm).

(C) Labeling of ventral roots in *P_0-creER^{T2}:Rosa26-YFP* mice provides an internal control for recombination efficiency. Although there is abundant Periaxin immunoreactivity in both the ventral roots and remyelinating lesions in the ventral funiculus at 21 dpl, YFP immunoreactivity is largely confined to the ventral root (scale bar represents 100 μm).

(D) At 21 dpl in *Pdgfra-creER^{T2}:Rosa26-YFP* or *Olig2-Cre:Rosa26-YFP* mice, there is extensive overlap of Periaxin and YFP immunoreactivity within remyelinating lesions but

no overlap in the ventral roots (VR). The converse situation is found in *P_0-creER^{T2}:Rosa26-YFP* mice; there is very little overlap between Periaxin and YFP within demyelinated lesions (arrows) whereas nearly all Periaxin$^+$ cells in the ventral roots are YFP$^+$ (scale bars represent 50 μm).

Europe PMC Funders Author Manuscripts

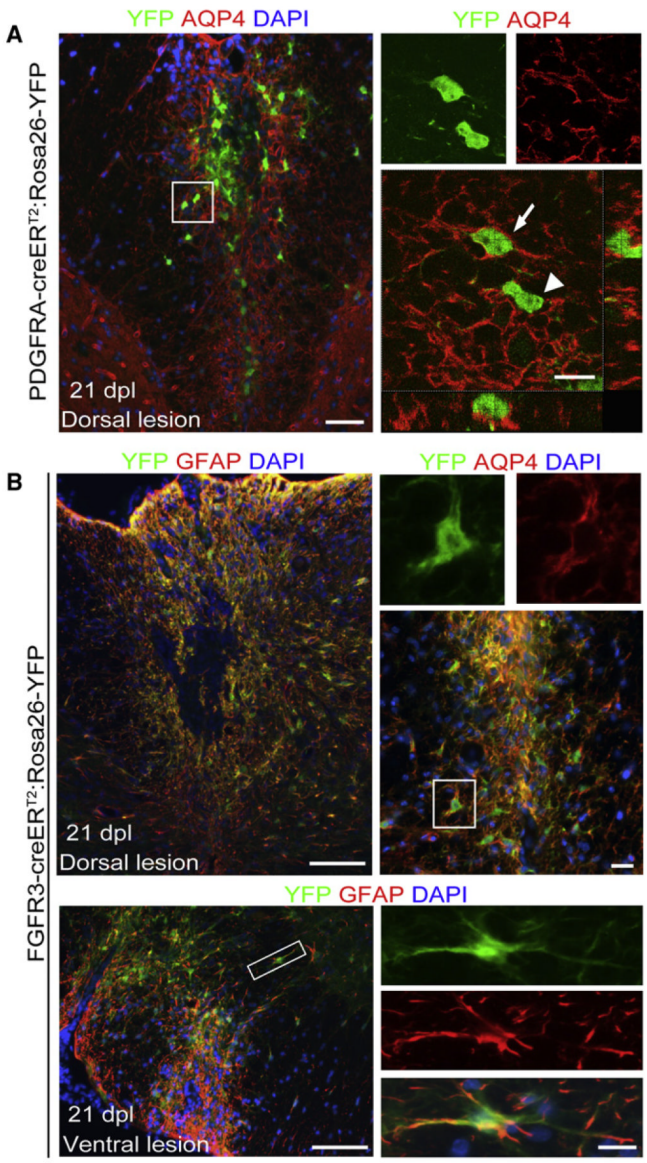

Figure 7. PDGFRA^{+} Precursors Give Rise to Limited Number of Astrocytes in the Lesion, usually within the Outer Rim of the Lesion

(A) Low-power micrograph of a dorsal lesion immunolabelled for YFP and AQP4 (scale bar represents 50 μm). A cell with a YFP^{+} cytoplasm that also expresses AQP4 on its surface (arrow; scale bar represents 10 μm) can easily be distinguished from an AQP4-negative cell (arrowhead).

(B) The majority of AQP4^{+} astrocytes within the lesion are derived from FGFR3^{+} cells as shown by double immunolabelling for YFP and either GFAP or AQP4 in dorsal or ventral lesions (scale bars represent 100 μm in main image, 20 μm in higher-magnification images of areas indicated by boxes).